

Characterization of the Nonequilibrium Steady State of a Heterogeneous Nonlinear q -Voter Model with Zealotry

ANDREW MELLOR¹, MAURO MOBILIA¹ and R.K.P. ZIA^{2,3}

¹ *Department of Applied Mathematics, School of Mathematics, University of Leeds, Leeds LS2 9JT, UK*

² *Department of Physics & Astronomy, Iowa State University, Ames, IA 50011, USA*

³ *Department of Physics, Virginia Polytechnic Institute & State University, Blacksburg, VA 24061, USA*

PACS 89.75.-k – Complex systems

PACS 02.50.-r – Probability theory, stochastic processes, and statistics

PACS 05.40.-a – Fluctuation phenomena, random processes, noise, and Brownian motion

Abstract – We introduce an heterogeneous nonlinear q -voter model with zealots and two types of susceptible voters, and study its *non-equilibrium* properties when the population is finite and well mixed. In this two-opinion model, each individual supports one of two parties and is either a zealot or a susceptible voter of type q_1 or q_2 . While here zealots never change their opinion, a q_i -susceptible voter ($i = 1, 2$) consults a group of q_i neighbors at each time step, and adopts their opinion if all group members agree. We show that this model violates the detailed balance whenever $q_1 \neq q_2$ and has surprisingly rich properties. Here, we focus on the characterization of the model's non-equilibrium stationary state (NESS) in terms of its probability distribution and currents in the distinct regimes of low and high density of zealotry. We unveil the NESS properties in each of these phases by computing the opinion distribution and the circulation of probability currents, as well as the two-point correlation functions at unequal times (formally related to a “probability angular momentum”). Our analytical calculations obtained in the realm of a linear Gaussian approximation are compared with numerical results.

Introduction. – Since Schelling's pioneering work [1] there has been increasing interest in using simple theoretical models to describe social phenomena such as the dynamics of opinions [2]. In this context, individual-based models commonly used in statistical physics are particularly insightful, as they reveal the micro-macro connection in social dynamics [1, 2]. The voter model (VM) [3] serves as a reference to describe the evolution of opinions in socially interacting populations. (See *e.g.* [2, 4] and references therein.) In spite of its paradigmatic role, the VM relies on a number of unrealistic assumptions, such as the total lack of self-confidence of all voters and their perfect conformity, which invariably leads to a consensus. In fact, it has been shown that members of a society respond differently to stimuli and this greatly influences the underlying social dynamics [5–7]. An approach to model a population with different levels of confidence is to assume that some agents are “zealots” who favor one opinion [8] or maintain a fixed opinion [9]. Since the introduction of these simple types of behavior in the VM, a large variety of zealot models have been studied, see, *e.g.*, Refs. [10].

In this Letter, we focus on a variant of the VM known as the two-state nonlinear q -voter model (q VM) [11] which has attracted much interest [12]. In the q VM, a voter can be influenced by a group of q neighbors. The version with $q = 2$ is closely related to the well-known models of Refs. [13]. Motivated by important psychology and sociology tenets [5, 6], the basic ideas underlying the q VM and zealotry have been combined into the q -voter model with *inflexible* zealots (q VMZ) [14]. Indeed, social scientists have established that conformity by imitation, an important mechanism for collective actions, is observed only when the group-size is large and can be altered by individuals who are able to resist the group pressure [6, 7]. It is understandable that social conformity is unlikely for small groups and can be significantly suppressed by the presence of zealots. In the q VMZ dynamics, both group-size limited conformity and zealotry are accounted for. Furthermore, in a well-mixed setting, this dynamics obeys detailed balance, so that the exact stationary distribution is easily found [14]. The system resembles one in thermal equilibrium, characterized by two phases: As zealotry is low-

ered through a critical level, the opinion distribution transitions from being single-peaked to being bimodal, with non-trivial switching dynamics (in finite populations).

Unlike in the models described above, the populations in our society are highly heterogeneous. In principle, we may describe the relevant situation of different responses to social stimuli by considering a distribution of q 's [5]. Does this generalization modify the conclusions of the q VMZ? If so, how? In this Letter, we explore the simplest way to this broader view, namely, a population with just two subgroups with different q 's (denoted by $2q$ VZ): $q_1 < q_2$. Similar to the q VMZ, phase transitions exist in the $2q$ VZ. Unlike in q VMZ, the dynamics of this model does not obey detailed balance, so the system relaxes into a non-equilibrium steady state (NESS). Thus, from the standpoint of statistical physics, $2q$ VZ is a highly non-trivial extension. In general, there is no simple way to compute a NESS distribution [15], while persistent probability current prevails [16]. As a consequence, there are observable quantities which are trivially zero in the q VMZ that do *not* vanish in the $2q$ VZ. For example, opinions among those with smaller q change more readily, and “drive” those in the other subgroup. Though subtle, directed “oscillations” associated with fluctuating quantities can be measured. Here, we report results of a baseline study with the simplest case $q_{1,2} = 1, 2$. Our methods include stochastic simulations and numerical solutions of the master equation for systems finite size N , as well as a continuum version based on the Fokker-Planck equation and its analysis through a linear Gaussian approximation (LGA) [16–19].

Model specification and NESS. – Our model, the $2q$ VZ, consists of a population of N voters who support one of two parties, the opinion of each denoted by ± 1 . Some voters are inflexible zealots, never changing their opinions. Their numbers are denoted by Z_{\pm} , the subscript showing the associated opinion. The rest are swing voters of two types, denoted by q_1 and q_2 . Known as q_i -susceptibles, their numbers are S_i , with $i = 1, 2$. During the evolution, each agent maintains its behavior, so that Z_{\pm} and S_i are all conserved (with $S_1 + S_2 + Z_+ + Z_- = N$). At each time step, a voter is chosen at random and if it is a zealot then no action is taken. However, if a q_i -susceptible is chosen, then it collects the opinions from a random group of q_i neighbors and adopts the opinion of the group only if their opinion is *unanimous*¹ (see supplementary material (SM) [20]). For simplicity, we investigate this model on a complete graph (well-mixed population). Since there is no spatial structure, our system is completely specified by the number n_i of q_i -susceptible voters holding opinion $+1$ (also denoted by $\vec{n} = (n_1, n_2)$).

Since configuration space is a discrete set of $S_1 \times S_2$ points and updates involve a single step to a nearest neigh-

bour on a square lattice, our system behaves exactly as a two-dimensional random walker, with inhomogeneous and biased rates. Thus, our simulation runs consist of recording the trajectories of such a random walker. Meanwhile, the full stochastic process is defined by a master equation (ME) for the evolution of $P(\vec{n}; T)$ [21], the probability to find our system in state \vec{n} , T time steps (attempts) after some initial configuration \vec{n}_0 . Since our main interest is the stationary distribution, $P^*(\vec{n})$, we suppress references to \vec{n}_0 . As T increases by unity, a walker at \vec{n} steps to \vec{n}' with probability $W(\vec{n} \rightarrow \vec{n}')$, a process represented by the ME $P(\vec{n}; T+1) = \sum_{\vec{n}'} \mathcal{G}(\vec{n}, \vec{n}') P(\vec{n}'; T)$. Here, $\vec{n}' \in \{(n_1 \pm 1, n_2), (n_1, n_2 \pm 1)\}$ is one of the four nearest neighbors of \vec{n} , from which the transitions occur with respective stepping probabilities $W_1^{\pm}(\vec{n})$ and $W_2^{\pm}(\vec{n})$:

$$W_i^+(\vec{n}) = \frac{S_i - n_i}{N} \left(\frac{Z_+ + n_1 + n_2}{N - 1} \right)^{q_i} \quad (1)$$

$$W_i^-(\vec{n}) = \frac{n_i}{N} \left(\frac{Z_+ + S_1 + S_2 - n_1 - n_2}{N - 1} \right)^{q_i}. \quad (2)$$

From here, it is straightforward to write an explicit form for \mathcal{G} , as well as joint probabilities $\mathcal{P}(\vec{n}, T; \vec{n}', T')$ at two different times². Much of our attention here will be devoted to the change, $P(\vec{n}; T+1) - P(\vec{n}; T)$, given by a sum of *probability currents* which account for transitions into, or out-of, the configuration \vec{n} . Specifically, the *net* probability current from \vec{n} to $\vec{n}' \equiv (n_1 + 1, n_2)$ is $K_1(\vec{n}; T) = W_1^+(\vec{n})P(\vec{n}; T) - W_1^-(\vec{n}')P(\vec{n}'; T)$, and a similar expression for $K_2(\vec{n}; T)$ for \vec{n} to $(n_1, n_2 + 1)$. Thus, $\mathcal{G}P$ is intimately related to the current $\vec{K} = (K_1, K_2)$.

To verify that this dynamics violates detailed balance (and time reversal), we may apply the Kolmogorov criterion [23] on any closed loop, the simplest being four \vec{n} 's around a plaquette [22]. As a consequence, our system settles into a NESS, with non-trivial P^* and stationary current \vec{K}^* . Though the main behavior of our model is qualitatively the same as in the q VMZ, the presence of \vec{K}^* leads to important, distinguishing features, displayed through physical observables, such as means, $\langle n_i \rangle \equiv \sum_{\vec{n}} n_i P^*(\vec{n})$, and correlations, $\langle n_i n_j \rangle_T \equiv \sum_{\vec{n}, \vec{n}'} n'_i n'_j \mathcal{P}^*(\vec{n}, T; \vec{n}', 0)$. Note that the order of indices in the latter is crucial: i (j) is associated with the earlier (later) variable when $T > 0$. One key observable is the *antisymmetric* part of $\langle n_i n_j \rangle_{T \neq 0}$. Being odd under time reversal, it highlights the underlying NESS characteristic, and so, vanishes in the q VMZ. When the time difference is infinitesimal ($T = 1$, large N), it can be identified as the total “probability angular momentum” [24], in analogy with the classical angular momentum associated with current loops in fluids. To illustrate these novel features, we examine in detail a specific model – $Z_+ = Z_-$, $S_1 = S_2$, $q_{1,2} = 1, 2$ – and provide several explicit results below.

¹ As in Refs. [11, 12, 14], we allow repetition. Note that in Ref. [11] a voter can change its opinion with a flip rate ϵ even in the absence of consensus among its q neighbors. Here, as in most of Refs. [12, 14], we set $\epsilon = 0$.

² Assuming $T > T'$, $\mathcal{P}(\vec{n}, T; \vec{n}', T') = \mathcal{G}^{T-T'}(\vec{n}, \vec{n}') P(\vec{n}', T')$. Details will be provided in [22].

Analytic results & simulation studies . –

Mean-field Approximation (MFA): This approach offers the most intuitive picture, valid when $N \rightarrow \infty$ with fixed densities: $(z_{\pm}, s_i, x_i) = (Z_{\pm}, S_i, n_i)/N$ (continuous variables subjected to $z_+ + z_- + s_1 + s_2 = 1$ and $x_i \in [0, s_i]$). In this limit, the rates W_i^{\pm} become $w_i^+(\vec{x}) = (s_i - x_i)\mu^{q_i}$ and $w_i^-(\vec{x}) = x_i(1 - \mu)^{q_i}$, where $\mu \equiv z_+ + x_1 + x_2$ clearly represents the fraction holding opinion +1. In the MFA, averages of products are replaced by products of averages, and from the ME, we find the rate equations (REs)

$$\dot{x}_i \equiv \partial_t x_i = w_i^+ - w_i^- = (s_i - x_i)\mu^{q_i} - x_i(1 - \mu)^{q_i}. \quad (3)$$

As in the q VMZ [14], the REs admit one or three fixed points, depending on z_{\pm} . At the fixed point(s), x_i^* , the ratio $\rho \equiv \mu^*/(1 - \mu^*)$ satisfies $z_+ + \sum_{i=1,2} s_i/(1 + \rho^{q_i}) = 1/(1 + \rho)$, while $x_i^* = s_i/(1 + \rho^{q_i})$. For models with $z_+ = z_-$, $\rho = 1$ is always a solution, associated with the symmetric fixed point $x_i^* = s_i/2$ (denoted by $\vec{x}^{(0)}$ below). Above a critical density of zealots, z_c , this is the only fixed point and is stable. For $z < z_c$, $\vec{x}^{(0)}$ turns unstable, while two others (denoted by $\vec{x}^{(\pm)}$) emerge and both are stable.

For our specific model ($z_{\pm} = z$, $s_i = s = 1/2 - z$, $q_i = i$), the MFA for z_c is $1/6$ (i.e., $s_c = 1/3$). When $z < z_c$, $\vec{x}^{(\pm)}$ are given by the two solutions to $\rho + (1/\rho) + 1 = 1/(2z)$, associated with the spontaneously breaking of the Ising-like symmetry ($\rho \Leftrightarrow 1/\rho$). Thus, this MFA predicts the same phase transition as in the q VMZ (pitchfork bifurcation [14]). Of course, being deterministic, it cannot account for fluctuations.

Fokker-Planck equation (FPE): In finite populations, demographic fluctuations are important, as they drive interesting time-dependent phenomena in the stationary state. For large but finite N , these fluctuations are embodied in the *probability density* $P(\vec{x}; t)$, the continuum version of $P(\vec{n}; T)$. Here, $t \equiv T/N$ also becomes continuous, as $P(\vec{n}; T+1) - P(\vec{n}; T) \rightarrow N^{-1} \partial_t P(\vec{x}; t)$. To the leading, non-trivial order in $1/N$, the evolution is adequately captured by the FPE: $\partial_t P(\vec{x}; t) = \sum_{i=1,2} \frac{\partial}{\partial x_i} \left[\frac{\partial}{\partial x_i} u_i(\vec{x}) P + v_i(\vec{x}) P \right]$ [21], where $u_i \equiv (w_i^+ + w_i^-)/2N$ and $v_i \equiv w_i^- - w_i^+$. Clearly, the right-hand-side can be identified as the divergence of the *probability current density*

$$K_i(\vec{x}; t) = -\partial [u_i P] / \partial x_i - v_i P$$

(continuum version of $K_i(\vec{n}; T)$). The stationary probability density $P^*(\vec{x})$ is given by $0 = \vec{\nabla} \cdot \vec{K}^*$. For a dynamics which satisfies detailed balance, \vec{K}^* necessarily vanishes, leading to equations for P^* that can be easily solved [21]. In a NESS, $\vec{K}^* \neq 0$, i.e., non-trivial currents persist. Clearly, the curl of \vec{K}^* does not vanish and, known in fluid dynamics as the vorticity, $\vec{\nabla} \times \vec{K}^*$ is a one-component field in two dimensions. Of course, \vec{K}^* can also be expressed as the curl of another field, the stream function. (See [20] for some details). In other words, the

currents form closed loops, which lead us to identify

$$L_{ij} = \int_{\vec{x}} [x_i K_j^*(\vec{x}) - x_j K_i^*(\vec{x})] d\vec{x} \quad (4)$$

as the total ‘*probability angular momentum*’ [24], by formal analogy with the total mass angular momentum $(\int_{\vec{x}} \vec{x} \times \vec{J} d\vec{x})$ in fluids with current density \vec{J} . As a pseudotensor in arbitrary dimensions, L_{ij} has just a single independent component, (say) $L_{12} = \mathcal{L}$. Since \vec{K}^* is linear in P^* , we identify \mathcal{L} as the steady state average of a function of \vec{x} . Below we show that the simple approximation $\vec{K}^* \propto \vec{x} P^*$ provides many analytic results, e.g., an expression for the two-point correlation at *unequal times* ³

$$C_{ij}(\tau) \equiv \langle x_i x_j \rangle_{\tau} \quad (\text{for } \tau \neq 0). \quad (5)$$

Decomposing C_{ij} into the symmetric and antisymmetric parts, we see that $\tilde{C}_{ij} \equiv C_{ij} - C_{ji}$ is *odd* in τ , highlighting time reversal violation and serving as a principal characteristic of a NESS. Indeed, to lowest order (in \vec{x}), L_{ij} is given by $\partial_{\tau} \tilde{C}_{ij}|_0$.

Linear Gaussian Approximation (LGA): In this scheme, we consider *deviations* from a fixed point, $\vec{\xi} \equiv \vec{x} - \vec{x}^*$, and, keeping the lowest non-vanishing order, we find the linearized version of the FPE [21]

$$\partial_t P(\vec{\xi}, t) = \sum_{i,j} \partial^i \left\{ D_{ij} \partial^j + F_i^j \xi_j \right\} P(\vec{\xi}, t), \quad (6)$$

where $\partial^i \equiv \partial/\partial \xi_i$, $D_{ij} = \delta_{ij} w_i^*/N$ with $w_i^* = w_i^+(\vec{x}^*) = w_i^-(\vec{x}^*)$, and $F_i^j \equiv -(\partial x_i / \partial x_j)|_{\vec{x}=\vec{x}^*}$ is the linear stability matrix at \vec{x}^* . Thus, the LGA is defined by two matrices: D_{ij} and F_i^j , or \mathbb{D} and \mathbb{F} for short. This linearized FPE can be translated into Langevin equations with linear drift $-\mathbb{F}\vec{\xi}$ plus Gaussian white noise controlled by \mathbb{D} [21]. Below we show that the LGA provides much insight into the non-equilibrium character of our model by allowing us to find analytic expressions for various quantities. From the explicit expressions [20], we find that $\det \mathbb{F} \propto 1 - 6z$ (in all cases) and its eigenvalues, denoted by λ_{\pm} , are positive in the regions of interest. Also expected, \mathbb{D} is $O(1/N)$, so that fluctuations of $\vec{\xi}$ are $O(1/\sqrt{N})$, and we note that $D_{11} > D_{22}$ which confirms that the q_1 -susceptibles are more likely to change their opinions.

If $\mathbb{D}^{-1}\mathbb{F}$ is symmetric, then detailed balance is satisfied and $P^* \propto \exp \left\{ -\vec{\xi} \mathbb{D}^{-1} \mathbb{F} \vec{\xi} / 2 \right\}$ is a Gaussian distribution for which $\mathbb{D}^{-1}\mathbb{F}/2$ is the ‘potential’. Here, we find that $\mathbb{D}^{-1}\mathbb{F}$ is *not* symmetric. Nevertheless, the solution of (6) is still a Gaussian [16–19]: $P^*(\vec{\xi}) \propto \exp \left(-\vec{\xi} \mathbb{C}^{-1} \vec{\xi} / 2 \right)$, where the elements of \mathbb{C} are $\langle \xi_i \xi_j \rangle_0$, the truncated $C_{ij}(0)$ ⁴. It can be expressed in terms of the eigenvectors and eigenvalues of \mathbb{F} [16, 17], or by solving $\mathcal{S}[\mathbb{F}\mathbb{C}] = \mathbb{D}$ [18, 19], where

³ Also known as the lagged correlation or lagged covariance.

⁴ $\langle \xi_i \xi_j \rangle_0 \equiv \langle x_i x_j \rangle_0 - \langle x_i \rangle \langle x_j \rangle = C_{ij}(0) - \langle x_i \rangle \langle x_j \rangle$.

$\mathcal{S}[\mathbb{F}\mathbb{C}]$ denotes the *symmetric part* of $\mathbb{F}\mathbb{C}$. Deferring the explicit forms of \mathbb{C} to elsewhere [22], we present here the implications for \vec{K}^* and the physical observables.

Since $\vec{\xi}P^* = -\mathbb{C}\vec{\partial}P^*$, the steady currents in Eq. (6) can be written as $\vec{K}^* = [\mathbb{F}\mathbb{C} - \mathbb{D}]\vec{\nabla}P^*$ [16]. We emphasize that, given $\mathcal{S}[\mathbb{F}\mathbb{C}] = \mathbb{D}$, the matrix $\mathbb{F}\mathbb{C} - \mathbb{D}$ is precisely the *antisymmetric part* of $\mathbb{F}\mathbb{C}$, here denoted by $\mathcal{A}[\mathbb{F}\mathbb{C}]$. Thus, \vec{K}^* is manifestly divergence free.

Proceeding to observables, we consider L_{ij} or simply, \mathbb{L} . Since $\int_{\vec{x}} \vec{K}^* d\vec{x} = 0$, the \vec{x} in Eq. (4) can be replaced by $\vec{\xi}$. In the framework of the LGA, we readily find the remarkably simple expression $\mathbb{L} = 2\mathcal{A}[\mathbb{F}\mathbb{C}]$. In this setting, we see that $\mathbb{F}\mathbb{C} = \mathbb{D} + \mathbb{L}/2$, placing this angular momentum on an equal footing with diffusion⁵. In our specific $2qVZ$, the only independent component is \mathcal{L} , given by $s^2/[(6-8s)N]$ and $4z^2/[(2z+3)N]$ for $\vec{x}^{(0)}$ and $\vec{x}^{(\pm)}$, respectively. Further, we recall that \mathbb{L} is intimately related to the two-point correlation $\mathbb{C}(\tau) \equiv \langle \xi_i \xi_j \rangle_\tau$ ⁶. In the LGA, $\mathbb{C}(\tau)$ is explicitly $\mathbb{C} \exp(-\mathbb{F}^T \tau)$ [19]. Here, its antisymmetric part is just one independent quantity and so, we focus on (say) $\tilde{C}_{12}(\tau)$. Dropping the subscript, we find the explicit expression

$$\tilde{C}(\tau) = \mathcal{L} \left(\frac{e^{-\lambda_- \tau} - e^{-\lambda_+ \tau}}{\lambda_+ - \lambda_-} \right) \quad (7)$$

which exposes some noteworthy features: Clearly, $\partial_\tau \tilde{C}(\tau)|_0 = \mathcal{L}$. Moreover, its long time behavior is governed by λ_- , the smallest eigenvalue of \mathbb{F} . Unlike typical correlations at unequal times, $\tilde{C}(\tau)$ is non-monotonic, with a peak at $\hat{\tau} = (\lambda_+ - \lambda_-)^{-1} \ln(\lambda_+/\lambda_-)$.

Below we show that all these predictions by the LGA are borne out in simulations and exact numerical results (for appropriate regions). Since the LGA is formulated around a single fixed point, it clearly cannot describe double-peaked distributions or escape times. By contrast, near each peak, the reliability of the LGA improves in the limit of $N \rightarrow \infty$ with fixed $z \neq 0, z_c$.

Exact numerical solution: For systems with small S , numerical methods can be used to obtain P^* , by exploiting the relation $[\mathcal{G}(\vec{n}, \vec{n}')^\infty = P^*(\vec{n})$ (independent of \vec{n}'). For example, for $S = 30$, by iterating $\mathcal{G}^{2\tau} = \mathcal{G}^\tau \mathcal{G}^\tau$ just 64 times, we find changes at $\lesssim 10^{-20}$. Illustrated in Fig. 1(a,b) are heat maps (contour plots) on 30×30 grids for two cases: $Z = 20$ and 13 . Associated with above and below z_c , they clearly show the expected single *vs.* double peaked distributions. In the SM [20], we show this transition in $S = 50$ systems with many such plots compiled into a movie.

In Fig. 1a, we see that the contours resemble ellipses typical of Gaussian distributions. Two other prominent features are: (i) The width in n_1 is much smaller than

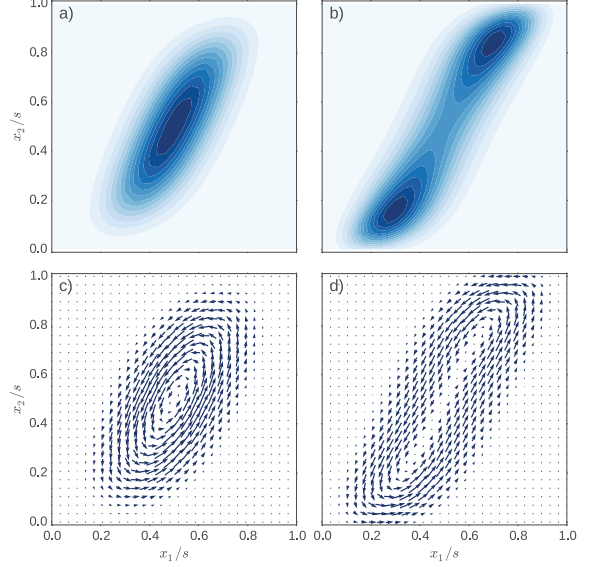


Fig. 1: (*Color online*). Stationary distribution and probability current obtained from the exact numerical solution of the ME in the high/low zealotry phase (left/right panels) with $S = 30$. Top: P^* as function of $\vec{x} = \vec{n}/N$; dark/light blue (grey) encodes a high/low probability. Bottom: The wind-field vectors represent \vec{K}^* at each point \vec{x} . Parameters are $Z = 20$ and $N = 100$ in (a, c), and $Z = 13$ and $N = 86$ in (b, d).

that in n_2 , indicative of the relative ease with which the q_1 -susceptibles change their opinion, so that they stay closer to the “center” typically. Since these widths scale with \sqrt{N} (≈ 10 here), we should expect only a qualitative fit from Gaussians. (ii) The alignment of the ellipses implies a strong correlation between the two variables, an expected result of both groups of susceptibles following the whims of the other.

In the $z < z_c$ case, we see that the q_2 -susceptibles display a larger spontaneous symmetry breaking than q_1 -voters, reflecting the same behavior as in the $qVMZ$. Meanwhile, if left alone, the q_1 -susceptibles would reach a coexistence state [9]. Thus, the broken symmetry in the opinion of the former acts as an external imbalance on the latter, dragging them to lean toward one pole or the other. Now, due to the strong finite size effects, the region around each peak appears quite asymmetric and seriously non-Gaussian when N is small. We also note that the peaks are linked via a “ridge”, the lowest point along which is often referred to as a “gap” by mountaineers. If we consider $-\ln P^*$, then this gap represents the lowest barrier between two “wells.” Also known as the saddle point, its height is expected to control the escape times faced by the random walker trapped in one or the other well. As we expect the height difference between the saddle and the well bottom to scale with N , we anticipate escape times to scale with e^N , as found in the $qVMZ$ [14]. Finally, note that the analysis of the critical region $z \cong z_c$ necessitates a detailed finite size scaling study, which is

⁵Note our distribution has unit “mass” ($\int P^* = 1$) so that the units of \mathbb{L} are x^2/t , precisely those of diffusion.

⁶Specifically, $\mathbb{L} = 2\mathcal{A}[\partial_\tau \mathbb{C}(\tau)|_0]$.

beyond the scope of this Letter.

From P^* , we have computed numerically other exact quantities of interest. The wind-field like plots of \vec{K}^* shown in Fig. 1(c,d) provide good impressions of the general counterclockwise swirl. Other characteristics (vorticity and stream function) are displayed in the SM [20]. More quantitatively, the physical observables are readily obtained and can be compared with the predictions of the LGA. Here, due to symmetry, the exact $\langle \vec{x} \rangle$ is $\vec{s}/2$, regardless of the location of the peak(s). The simplest non-trivial quantities are two point correlations (\mathbb{C}, \mathcal{L}) and we find that the predictions of the LGA are in qualitative agreement with exact calculations [20] in the high zealotry phase $z > z_c$. In principle, we access the exact decay constants (λ_{\pm}) by analyzing \mathcal{G}^T numerically, a task deferred to a future study [22]. In the low zealotry phase, $z < z_c$, we emphasize that P^* includes *all* trajectories, with visits near both $x^{(\pm)}$. Yet, the LGA can be expected to be good only around *one* of the two peaks. Hence, blindly computing \mathbb{C} or \mathcal{L} from this P^* will not allow us to compare them with the predictions of LGA. Indeed, it is a highly non-trivial task to interpret \mathcal{L} , since a detailed understanding of the contributions from tunneling is necessary. As for comparisons with simulations results, the key is whether the runs are long enough to permit a good sampling of both wells. In summary, while the LGA succeeds in capturing the essentials of the z systems here, the finite size effects are too large for good quantitative agreement. For $z < z_c$ cases, we expect that the predictive power of the LGA will improve when the zealotry is asymmetric since tunneling events then become extremely rare [14, 22].

Simulation studies: While the above methods yield exact results, they are restricted to small systems. To study larger N 's, we rely on stochastic simulations, based on running a random walker on a $S \times S$ lattice with the biased and inhomogeneous stepping probabilities (1,2), and performed using the Gillespie algorithm [25]. Using z 's not particularly close to either 0 or z_c , our runs are up to 10^8 steps, for systems as large as $N = 3600$. The entire trajectory of each run is recorded, giving us the time series $\vec{n}(T)$ and so, $\vec{x}(t)$ and $\xi(t)$. Examining these, we find that, within 1000 time steps of starting at $(0, 0)$, the walk appears to be in a steady state. With these traces, we can construct time averages and obtain $\langle \vec{x} \rangle$ and the general two-point correlation function $C_{ij}(\tau)$ in the NESS.

First, as a check, we collected data for the small systems discussed above ($S = 30$, with $Z = 20, 13$). For the former, we find the truncated $C_{ij}(0)$ to be $(C_{11}, C_{12}, C_{22}) = (1.74, 1.66, 3.53) \times 10^{-3}$. Further, we compile $\tilde{C}(\tau)$ and find the behavior predicted in Eq. (7), see Fig. 2. By fitting with this form, we find $\lambda_{\pm} = 0.833, 0.091$ and $\mathcal{L} \cong 2.16 \times 10^{-4}$. Both $C_{ij}(0)$ and \mathcal{L} are in excellent agreement (within 0.6%) with the exact result [20]. By contrast, the LGA predictions are qualitatively acceptable (from a few % to the right order of magnitude). For the $Z = 13$ case, the walker spends much of its time wandering back

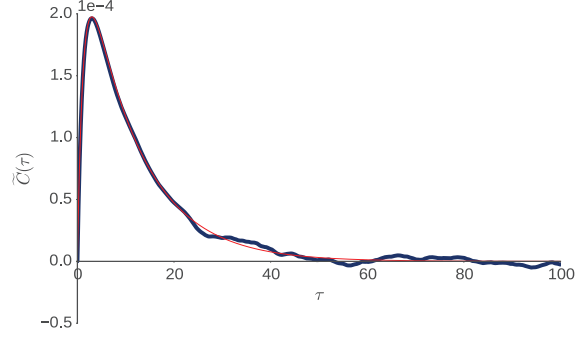


Fig. 2: (Color online). $\tilde{C}(\tau)$ vs. τ in the high zealotry phase, with $N = 100$, $Z = 20$, and $S = 30$: The results of simulations (black) obtained by sampling every 0.01 time step and averaged over 99×10^6 data points. Comparison with the LGA expression (7) with $\lambda_+ = 0.833$ and $\lambda_- = 0.091$ (red/grey), see text.

and forth between the wells, implying that P^* is attained. As a result, the findings for \mathbb{C} are also in excellent agreement (within 1%) with the exact results [20]. However, in this case the comparison with the LGA predictions is pointless, since the LGA is devised for just one well.

Turning to large systems, two examples ($Z = 400$ and 800 , $S = 1000$) are offered in the SM [20]. In the low zealotry case, the walker remains in *one well* for the entire run. Thus, it is meaningful to compare both sets of data with MFA/LGA predictions. For $z < z_c$, the simulation results of $\langle \vec{x} \rangle$ compares well with the MFA $\vec{x}^{(\pm)}$. In both cases, the data for the correlations $\langle n_i n_j \rangle_0$ and $\langle n_i n_j \rangle_1$ are in quantitatively good agreement with the LGA predictions for \mathbb{C} and \mathbb{FC} [20]. In summary, we have found that the LGA is indeed quite reliable for large S, Z (around each \vec{x}^*). Meanwhile, the various methods presented in this section all point to the presence of interesting new phenomena associated with the NESS aspect of $2qVZ$, namely, the presence of observable quantities odd under time reversal.

Summary and outlook. — In this Letter, we introduced a generalization of the $qVMZ$ (q -voter model with zealots) [14] which takes into account expected inhomogeneities in the behavior of swing voters and the presence of zealots. In arguably the simplest generalization of the $qVMZ$, we have just *two* groups of swing voters, distinguished by needing a consensus of q_1 or q_2 of its neighbors to adopt their opinion. As in Ref. [14], our model is characterized by two phases: When the fraction z of zealots is low, the long-time opinion distribution is bimodal whereas it is single-peaked when z is above a critical value z_c . However, a major and far-reaching difference between the $qVMZ$ and ours is that detailed balance is violated here. Hence, though the qualitative features are similar to those recently reported in [14], our system settles into a genuine NESS. As a result, there are persistent probability current loops which are odd under time reversal. We investigate these currents and some observ-

able manifestations thereof, in the simple but generic case $q_{1,2} = 1, 2$ with $S_1 = S_2$ and $Z_+ = Z_-$. Using numerical methods for small systems, Gaussian approximation for large ones, and simulation runs for both, we arrive at a comprehensive picture for our system. Quite remarkably, we show that this simple model exhibits stationary microscopic current loops (see Fig. 1), resulting in oscillations in certain macroscopic observables (e.g., the antisymmetric part of the two-point correlation function at unequal times, see Fig. 2). While the detailed relationships between microscopic probability currents and macroscopic social phenomena remain to be explored, our study clearly points to the presence, albeit subtle, of predator-prey like oscillations. The overall counter-clockwise flow in \vec{K}^* implies that fluctuations in the q_2 -susceptibles follow those of the other group, much like the population of lynxes follow those of hares. We believe this stems from the presence of “leaders” and “followers” in a society. Clearly, this study provides only the initial steps towards a systematic investigation of multi- q VM’s, which are expected to display other interesting phenomena. For this particular model, much more can be examined, e.g., finite size effects, scaling properties near z_c , and full distributions of \mathcal{L} [24]. Beyond studying the $2qVZ$ and similarly tractable models, the goal of our long-term efforts is to explore fundamental issues of NESS, in an attempt to formulate an overarching framework for non-equilibrium statistical mechanics.

We are grateful to B Schmittmann and J B Weiss for enlightening discussions. This research is supported partly by a US National Science Foundation grant: OCE-1245944. The support of the UK EPSRC and Bloom Agency (Leeds, UK) via a CASE Studentship to AM is gratefully acknowledged (Grant EP/L50550X/1).

REFERENCES

- [1] SCHELLING T. C., *Micromotives & Macrobbehavior* (WW Norton & Company) 2006.
- [2] CASTELLANO C., FORTUNATO S. and LORETO V., *Reviews of Modern Physics*, **81** (2009) 591.
- [3] LIGGETT T. M., *Interacting Particle Systems* (Springer) 1985.
- [4] GALAM S., *Sociophysics: A Physicist’s Modeling of Psycho-political Phenomena* (Springer Science & Business Media) 2012; SEN P. and CHAKRABARTI B. K., *Sociophysics: An Introduction* (Oxford University Press) 2013.
- [5] GRANOVETTER M., *American Journal of Sociology*, **83** (1978) 1420.
- [6] LATANÉ B., *American Psychologist*, **36** (1981) 343.
- [7] ASCH S. E., *Scientific American*, **193** (1955) 35; MILGRAM S., BICKMAN L. and BERKOWITZ L., *Journal of Personality and Social Psychology*, **13** (1969) 79.
- [8] MOBILIA M., *Physical Review Letters*, **91** (2003) 028701; MOBILIA M. and GEORGIEV I. T., *Physical Review E*, **71** (2005) 046102.
- [9] MOBILIA M., PETERSEN A. and REDNER S., *Journal of Statistical Mechanics: Theory and Experiment*, **2007** (2007) P08029.
- [10] GALAM S. and JACOBS F., *Physica A: Statistical Mechanics and its Applications*, **381** (2007) 366; SZNAJD-WERON K., TABISZEWSKI M. and TIMPANARO A. M., *EPL (Europhysics Letters)*, **96** (2011) 48002; XIE J., SREENIVASAN S., KORNISS G., ZHANG W., LIM C. and SZYMANSKI B. K., *Physical Review E*, **84** (2011) 011130; MASUDA N., *Scientific Reports*, **2** (2012) ; ACEMOGLU D., COMO G., FAGNANI F. and OZDAGLAR A., *Mathematics of Operations Research*, **38** (2013) 1; NYCZKA P. and SZNAJD-WERON K., *Journal of Statistical Physics*, **151** (2013) 174; WAAGEN A., VERMA G., CHAN K., SWAMI A. and D’SOUZA R., *Physical Review E*, **91** (2015) 022811; ARENDT D. L. and BLAHA L. M., *Computational and Mathematical Organization Theory*, **21** (2015) 184; MASUDA N., *New Journal of Physics*, **17** (2015) 033031; BORILE C., MOLINA-GARCIA D., MARITAN A. and MUÑOZ M. A., *Journal of Statistical Mechanics: Theory and Experiment*, (2015) P01030; MOBILIA M., *Chaos, Solitons & Fractals*, **56** (2013) 113; MOBILIA M., *Physical Review E*, **86** (2012) 011134; MOBILIA M., *Physical Review E*, **88** (2013) 046102; MOBILIA M., *Journal of Statistical Physics*, **151** (2013) 69.
- [11] CASTELLANO C., MUÑOZ M. A. and PASTOR-SATORRAS R., *Physical Review E*, **80** (2009) 041129.
- [12] SLANINA F., SZNAJD-WERON K. and PRZYBYŁA P., *EPL (Europhysics Letters)*, **82** (2008) 18006; GALAM S. and MARTINS A. C., *EPL (Europhysics Letters)*, **95** (2011) 48005; PRZYBYŁA P., SZNAJD-WERON K. and TABISZEWSKI M., *Physical Review E*, **84** (2011) 031117; NYCZKA P., CISŁO J. and SZNAJD-WERON K., *Physica A: Statistical Mechanics and its Applications*, **391** (2012) 317; TIMPANARO A. M. and PRADO C. P., *Physical Review E*, **89** (2014) 052808; JĘDRZEJEWSKI A., CHMIEL A. and SZNAJD-WERON K., *Physical Review E*, **92** (2015) 052105.
- [13] SZNAJD-WERON K. and SZNAJD J., *International Journal of Modern Physics C*, **11** (2000) 1157; LAMBIOTTE R. and REDNER S., *EPL (Europhysics Letters)*, **82** (2008) 18007.
- [14] MOBILIA M., *Physical Review E*, **92** (2015) 012803.
- [15] HILL T. L., *Journal of Theoretical Biology*, **10** (1966) 442.
- [16] ZIA R.K.P. and SCHMITTMANN B., *Journal of Statistical Mechanics: Theory and Experiment*, (2007) P07012.
- [17] LAX M., *Reviews of Modern Physics*, **38** (1966) 541.
- [18] WEISS J. B., *Tellus A*, **55** (2003) 208.
- [19] WEISS J. B., *Physical Review E*, **76** (2007) 061128.
- [20] MELLOR A., MOBILIA M. and ZIA R.K.P., Figshare (2016), Supplementary Material: <https://dx.doi.org/10.6084/m9.figshare.2060595>
- [21] VAN KAMPEN N. G., *Stochastic Processes in Physics and Chemistry* Vol. 1 (Elsevier) 1992; GARDINER C. W. *et al.*, *Handbook of Stochastic Methods* Vol. 3 (Springer Berlin) 1985.
- [22] MELLOR A., MOBILIA M. and ZIA R.K.P., *In preparation*.
- [23] KOLMOGOROV A., *Math. Ann.*, **112** (1936) 155.
- [24] SHKARAYEV M. S. and ZIA R., *Physical Review E*, **90** (2014) 032107.
- [25] GILLESPIE D. T., *The Journal of Physical Chemistry*, **81** (1977) 2340.